576-34

82241

Droplet Deformation in an Extensional Flow: The Role of Surfactant Physical Chemistry

Kathleen J. Stebe, Chemical Engineering Department, Johns Hopkins University, Baltimore, MD 21218

6

Abstract

Surfactant-induced Marangoni effects strongly alter the stresses exerted along fluid particle interfaces. In low gravity processes, these stresses can dictate the system behavior. The dependence of Marangoni effects on surfactant physical chemistry is not understood, severely impacting our ability to predict and control fluid particle flows. A droplet in an extensional flow allows the controlled study of stretching and deforming interfaces. The deformations of the drop allow both Marangoni stresses, which resist tangential shear, and Marangoni elasticities, which resist surface dilatation, to develop. This flow presents an ideal model system for studying these effects.

Prior surfactant-related work in this flow considered a linear dependence of the surface tension on the surface concentration, valid only at dilute surface concentrations, or a non-linear framework at concentrations sufficiently dilute that the linear approximation was valid. [1-3] The linear framework becomes inadequate for several reasons. The finite dimensions of surfactant molecules must be taken into account with a model that includes surfaces saturation. Nonideal interactions between adsorbed surfactant molecules alter the partitioning of surfactant between the bulk and the interface, the dynamics of surfactant adsorptive/desorptive exchange, and the sensitivity of the surface tension to adsorbed surfactant. For example, cohesion between hydrocarbon chains favors strong adsorption. Cohesion also slows the rate of desorption from interfaces, and decreases the sensitivity of the surface tension to adsorbed surfactant. Strong cohesive interactions result in first order surface phase changes with a plateau in the surface tension vs surface concentration. Within this surface concentration range, the surface tension is decoupled from surface concentration gradients.

We are engaged in the study of the role of surfactant physical chemistry in determining the Marangoni stresses on a drop in an extensional flow in a numerical and experimental program. Using surfactants whose dynamics and equilibrium behavior have been characterized in our laboratory, drop deformation will be studied in ground-based experiment. In an accompanying numerical study, predictive drop deformations will be determined based on the isotherm and equation of state determined in our laboratory. This work will improve our abilities to predict and control all fluid particle flows.

Introduction

When an initially spherical drop suspended in an immiscible fluid is subject to an extensional flow, it elongates. The flow field is governed by Stokes' equations for an incompressible fluid, continuity of velocity, the interfacial stress balance, and a far-field imposed pure straining motion. In the absence of surfactant adsorption, two dimensionless groups determine the extent of the deformation; the viscosity ratio of the drop to the suspending phase λ, and the capillary number Ca, which is the ratio of characteristic viscous stresses, which tend to deform the drop, to surface tension, which resists deformation. For weak flows, (small Ca), the drop deforms only slightly from a spherical geometry.[4,5] As Ca increases, the steady shapes are more elongated. If the flow is strong enough (Ca in excess of a critical value Ca^{cr}), the drop will not attain a steady shape, but will continue to elongate and ultimately fragment into smaller drops. The viscosity ratio λ affects both the steady shapes observed and the values of Ca^{cr}. Drops of low viscosity ($\lambda << 1$) exhibit shapes that have pointed ends which break off into satellite drops, a phenomenon called "tip-streaming"; highly viscous drops have bulbous ends. The role of λ is well documented both theoretically [4,5] and experimentally [6-8].

Figure 1

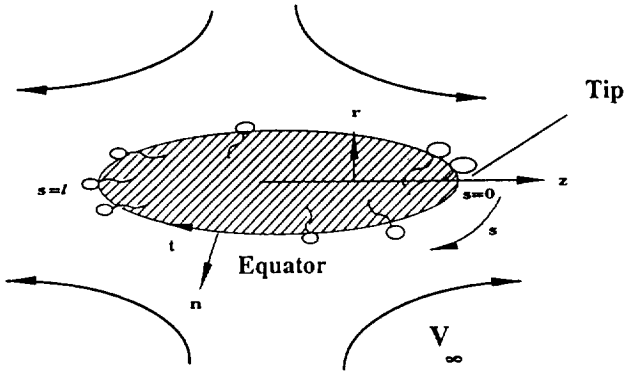

Surfactants present in either phase adsorb on the drop interface and reduce the surface tension. Their effect on the flow can be understood by considering the flow geometry, shown in Figure 1. An initially spherical drop with a uniform concentration of adsorbed surfactant is centered in an extensional flow which creates a stagnation ring at the drop equator and stagnation points at either tip. Surface convection sweeps adsorbed surfactant toward the poles. The resulting non-uniform surfactant distribution alters the interfacial stress balance: [9]

$$[\,[\boldsymbol{n}\cdot\underline{\boldsymbol{T}}]\,] = -\nabla_s\gamma\,\boldsymbol{t} + 2H\gamma\,\boldsymbol{n}$$

where $\underline{\mathbf{T}}$ is the Cauchy stress tensor, $\mathbf{n}$ is the surface normal, and the bracketed term on the left hand side of (1) represents the stress jump at the interface. The tangent vector to the surface is denoted $\mathbf{t}$, γ is the surface tension, ∇_s is the surface gradient operator, and 2H is the mean curvature of the interface. This expression can be made dimensionless by scaling the viscous stresses by μG, (where G is the applied strain rate, and μ is the viscosity of the external fluid), scaling lengths with the initial drop radius a, the surface tension with its value in equilibrium with the initial, uniform surface concentration $\gamma_{eq}(\Gamma_{eq})$, and using the chain rule to express the dependence of the surface tension on the surface concentration:

$$Ca\,[\,[\boldsymbol{n}\cdot(\underline{T}'-\lambda\hat{\underline{T}}']\,] = -E\left[\frac{\partial\gamma'}{\partial\Gamma'}\frac{1}{R'T'}\right]\nabla_s\Gamma'\boldsymbol{t} + 2H'\gamma'(\Gamma')\,\boldsymbol{n} \qquad (1)$$

The derivative of the surface tension with respect to the surface concentration is made dimensionless by RT, the product of the ideal gas constant and the temperature; Γ_∞ is the maximum surface packing of surfactant on the interface. Two dimensionless groups appear; Ca is the capillary number, E is a Gibbs elasticity number, a characteristic magnitude of the dependence of the surface tension on the surface concentration, defined as:

$$Ca = \frac{\mu G a}{\gamma_{eq}} \;;\; E = \frac{RT\Gamma_\infty}{\gamma_{eq}}$$

The greater is E, the more sensitive is the flow to non-equilibrium surfactant distributions.

These non-equilibrium distributions alter the flow is two ways. The interface will pull from the low surface tension zone at the poles toward the elevated tension at the equator, exerting a Marangoni stress which resists the viscous shear. In addition, since regions of low surface tension require higher curvatures to balance the normal stress jump across the interface, low tension regions become elongated and curved, leading to higher deformations in the surfactant-rich regions of the interface. This elongation serves to dilute the surface concentration, further perturbing the surfactant distribution. This is accompanied by a flattening of the surfactant-poor regions, which strongly resist surface dilatation. This effect in the normal stress balance is the Marangoni elasticity.

The surfactant distribution is determined by the relative rates of surface convection and surface dilatation, which disturb the surfactant distribution from equilibrium, to the rates of surface diffusion, bulk diffusion and adsorption-desorption, all of which tend to restore interfacial equilibrium. The diffusion and sorption kinetics are determined by the chemical structure of the surfactant and the bulk fluids. The surface tension dependence on the surface concentration is determined by the interfacial thermodynamics including the adsorption isotherm and the surface equation of state. Non-ideal interactions between surfactant molecules (e.g. cohesion or repulsion) strongly impact the form of these expressions [10,11] The required data are scarce in the literature. The measurement of these kinetic and thermodynamic parameters has been the emphasis of a recent studies in our laboratory.[12,13] The role of surface saturation and surfactant interactions has not been explored previously in terms of their impact in dynamic immiscible fluid systems. We are currently engaged in studying the role of the surfactant physical chemistry in drop deformation and break-up in a two part study. In the first part, the flow field is studied numerically. The location of the drop interface is not known *a priori*. A time-marching numerical scheme is employed starting from an initially spherical drop and tracing its shape evolution as a function of the capillary number, Ca, until either a steady drop shape is attained or the surface velocity diverges, indicating drop fragmentation. For work completed to date on bulk insoluble surfactants, (Pawar and Stebe, in press, Physics of Fluids) [14] the coupled Stokes' flow and mass transfer equations are solved numerically using the Boundary Element Method for the instantaneous velocity and an explicit Euler scheme to advance the surfactant distributions. Our results in this limit are briefly described. Future work will focus on bulk soluble surfactants with finite convective transport using the front tracking technique [15].

In the second part of the research, ground-based experiment is used to test the accuracy of these models

in predicting the drop shape evolution and break-up. Surfactant molecules which exhibit non-ideal interactions are identified as part of an ongoing project in our laboratory. Using these surfactants, we will measure the deformation of liquid drops in surfactant solutions in a computer-controlled four roll mill apparatus. Digitized images of the deforming drop are recorded. These images will be used to calculate the deformations as a function of Ca which will be compared with theoretical predictions.

Below, the relevant surfactant physical chemistry and dynamics, along with our insoluble surfactant work in this flow field are briefly reviewed. Thereafter, a brief discussion of the research objectives for the theoretical and experimental parts of this study is given.

Surfactant Mass Transfer

Non-uniform surfactant distributions develop when the rates of surface convection and dilatation which disturb the surfactant concentration Γ from equilibrium are rapid compared to the rate of surface diffusion and the rate that surfactant is supplied from the bulk fluid. The balance of these competing fluxes is given by: [16]

$$\frac{\partial \Gamma}{\partial t} + \nabla_s \cdot (\Gamma \boldsymbol{v_s}) - D_s \nabla_s^2 \Gamma = -\boldsymbol{n} \cdot \boldsymbol{j} \qquad (2)$$

where D_s is the surface diffusivity, and $\mathbf{v}_s$ is the surface velocity which has both a normal component which stretches the interface and a tangential component which sweeps surfactant along the surface.

The bulk concentration C is determined by the balance of convection and diffusion in the bulk:

$$D\nabla^2 C = \frac{\partial C}{\partial t} + \boldsymbol{v} \cdot \nabla C \qquad (3)$$

The normal flux of surfactant from the bulk to the interface takes place via two steps in series. Surfactant diffuses from the bulk to the fluid sublayer immediately adjacent to the interface. The diffusive flux toward an interface with normal **n** into the fluid is given by:

$$-\boldsymbol{n} \cdot \boldsymbol{j}_D = \boldsymbol{n} \cdot D \nabla C \big|_s \qquad (4)$$

where C is the bulk concentration, D is the diffusivity of the surfactant in solution, and the subscript s indicates that the flux is evaluated at the interface. Subsequently, surfactant adsorbs/desorbs from this sublayer onto the interface. Using a reaction-kinetic framework, the adsorptive-desorptive flux is given by:

$$-\boldsymbol{n} \cdot \boldsymbol{j}_{ads} = \beta e^{(-E_a/RT)} C_s (\Gamma_\infty - \Gamma) - \alpha e^{(-E_d/RT)} \Gamma \qquad (5)$$

The constants β [$cm^3 mol^{-1} s^{-1}$] and α [s^{-1}] are the kinetic constants for adsorption and desorption, respectively. The symbol Γ_∞ [mol cm^{-2}] is the maximum packing of surfactant along the interface, and Γ [mol cm^{-2}] denotes the surface concentration of adsorbed surfactant. The energy terms E_a and E_d [erg] are the energies of activation for adsorption and desorption, respectively, and RT is the product of the ideal gas constant and the absolute temperature.

Defining Γ' and C' as dimensionless surface and bulk concentrations scaled with their respective values at equilibrium, Γ_{eq} and C_{eq}, scaling time with the inverse rate of strain G^{-1}, and using the quantity $\Gamma_{eq}G$ to scale the flux from the bulk, the dimensionless bulk balance becomes:

$$\nabla^2 C' = Pe\left\{\frac{\partial C'}{\partial t'} + \boldsymbol{v}' \cdot \nabla C'\right\} \qquad (6)$$

The dimensionless surface mass balance is:

$$\frac{\partial \Gamma'}{\partial t'} + \nabla_s \cdot (\Gamma' \boldsymbol{v}_s') - \frac{1}{Pe_s} \nabla_s^2 \Gamma' = -\boldsymbol{n} \cdot \boldsymbol{j}' \qquad (7)$$

where the primes indicate a dimensionless quantity. The dimensionless normal flux expressions can be written:

$$-\boldsymbol{n} \cdot \boldsymbol{j}_D' = \frac{1}{h\,Pe} \boldsymbol{n} \cdot \nabla C' \qquad (8)$$

and

$$-\boldsymbol{n}\cdot\boldsymbol{J}'_{ads}=Bi\,(kC_s'(\frac{\Gamma_\infty}{\Gamma_{eq}}-\Gamma')-\Gamma') \qquad (9)$$

In these expressions, the following dimensionless groups appear:
(i.) The surface Peclet number, Pe_s and the bulk Peclet number Pe, which give the ratio of characteristic convective to surface diffusive or bulk diffusive fluxes, respectively.

$$Pe_s=\frac{a^2G}{D_s};\quad Pe=\frac{a^2G}{D}$$

(ii.) The adsorption depth, which is the depth beneath the interface depleted to populate the interface.

$$h=\frac{\Gamma_{eq}}{C_{eq}a}$$

(iii.) The Biot number, which is a measure of sorption rate to surface convective rate.

$$Bi=\frac{\alpha}{G}$$

(iv.) The adsorption number, which is the ratio of the characteristic rates of adsorption to desorption.

$$k=\frac{\beta C_{eq}}{\alpha}\exp^{-\frac{(E_a-E_d)}{RT}}$$

Mass Transfer Regimes to be Studied Numerically

In order to realistically model bulk soluble surfactants, the regime of finite Pe must be considered. This will be the focus of our numerical work. The ratio 1/hPe is the characteristic diffusive flux to the interface relative to the surface convective flux, and Bi is the adsorptive flux to convective flux. Therefore,

$$\eta=\frac{DC_{eq}}{\Gamma_{eq}a\alpha}$$

is the ratio of the characteristic diffusive to sorptive flux. The magnitude of this group determines the surfactant mass transfer regime. For fixed surfactant physical chemistry, these regimes can be spanned by varying the bulk concentration.

- $\eta\sim 0$, and the normal flux to the interface goes to zero. The surfactant behaves as an insoluble layer on the interface. Equation (7), with the right hand side set to zero governs Γ'. This limit has been explored in Pawar and Stebe.
- For small η the diffusive flux is rate limiting; C_s' is determined according to (6) and (8). Surfactant partitions instantaneously between the sublayer and the interface according to the adsorption isotherm $\Gamma'(C_s')$ obtained by setting (9) to zero.
- For η of O(1), the system has mixed kinetic-diffusion control. At finite Pe, diffusion and convection determine C' according to (6). The diffusive flux (8) determines C_s', and the sorption flux (9) regulates Γ'. These fluxes are equal, and give the right hand side of (7).
- Finally, for large η, the sorption flux (9) is rate controlling; diffusion instantaneously maintains C' at unity.

Non-ideal interactions among adsorbed surfactants

The energies terms that appear in the Arrhenius factor in (5) determine the form of the equilibrium adsorption isotherm obtained by setting (9) to zero. For example, if they are constant, the Langmuir adsorption isotherm is obtained. Through the Gibbs-Duhem equation for the interface, the corresponding surface equation of state is found.

For long chain saturated surfactants (e.g. the n-alcohols, [10]) the energies for adsorption and desorption

depend upon the surface concentration because of cohesive interactions among the saturated chains. For bulky sidechains, repulsive interactions have been observed. If this dependence is assumed to be linear,

$$E_i = E_{io} + \nu_i \Gamma_{eq} \tag{10}$$

where i =a,d respectively, the corresponding adsorption isotherm and surface equation of state are given by the Frumkin equations:

$$\frac{\Gamma_{eq}}{\Gamma_\infty} = \frac{k_f}{e^{\left(\frac{K\Gamma_{eq}}{\Gamma_\infty}\right)} + k_f} \tag{11}$$

$$\gamma = \gamma_o + RT\Gamma_\infty \left(\ln\left[1 - \frac{\Gamma_{eq}}{\Gamma_\infty}\right] - \frac{K}{2}\frac{\Gamma_{eq}^2}{\Gamma_\infty} \right) \tag{12}$$

where the adsorption constant is:

$$k_f = \frac{\beta C_{eq}}{\alpha} e^{\frac{-(E_{ao}-E_{do})}{RT}} \tag{13}$$

and the interaction parameter is:

$$K = \frac{(\nu_a - \nu_d)\Gamma_\infty}{RT} \tag{14}$$

which is negative for cohesion, i.e. as Γ increases, the energy required for surfactant to desorb also increases. For K=0, the surfactants have no non-ideal interactions, and the Langmuir case is recovered. In this expression, γ_0 and γ_{eq} are the surface tension of the clean interface and that in equilibrium with Γ_{eq}, respectively. These non-ideal interactions strongly alter the partitioning of surfactant between the bulk and the interface. For example, for a given C_{eq}, the $\Gamma_{eq}/\Gamma_\infty$ which result are greater for cohesion, and smaller for repulsion when compared to the Langmuir case. In addition, for a given Γ_{eq}, γ_{eq} reduces less for cohesion and more for repulsion relative to the Langmuir case. The comparison between the Frumkin and Langmuir frameworks is somewhat subtle in terms of C_{eq}, however, since surfactant partitioning is also effected.

For the case of cohesion, $\nu_d > 0$, and the net desorption coefficient as Γ increases:

$$\alpha_{eff} = \alpha(\Gamma=0) \exp^{\frac{-\nu_d \Gamma}{RT}}$$

slowing the effective Biot number, and thereby leading to more pronounced surface concentration gradients. The converse effect is expected for repulsive interactions.

The effect of the Γ distribution on the flow is determined by the surface equation of state. Figure 2 depicts the dimensionless surface pressure vs. a normalized area per molecule $\Gamma_{eq}^{-1}\Gamma_\infty$ for repulsion (K=2.52); no interactions, (K=0, Langmuir); for moderate cohesion (K=-2.52) and for the elevated cohesion (K=-4.0) case where an interface exhibits a significant flattening in the surface pressure-area per molecule isotherm. The case of stronger cohesion, where the interface undergoes a phase transition from a surface expanded to a condensed state is also shown. This requires a more sophisticated treatment of the equation of state. First order phase changes are discussed in the insoluble limit by Pawar and Stebe.

Droplet Deformation for Insoluble Surfactants with of Non-Ideal Interactions

One set of results from the study of Pawar and Stebe are briefly described here. At fixed surface concentration, the drop deformation is shown to vary with K in Figure 3 for an insoluble surfactant. Deformations are defined in terms of the drop length L and breadth B, and are plotted vs. Ca are diagrammed. First, compare the K=0 case which accounts for surface saturation to the linear framework. Saturation generates strong Marangoni stresses as surfactant is swept to the poles, preventing the surface concentration from attaining its maximum value. More uniform surface concentration profiles result, with reduced tip stretching when compared to the linear case.

Thus, smaller deformations are realized. For nonzero K, drop deformations were found to decrease with K, i.e. repulsive interactions gave the least deformations, while cohesive interactions between molecules gave the greatest.

Research Objectives

In the numerical part of the work, we will explore the role of repulsion/cohesion and strong cohesion resulting in surface phase changes for bulk soluble surfactants with diffusion control or mixed kinetic-diffusion control at finite Pe. The aim of the experimental aspect of the research program is to investigate whether the trends predicted by the theoretical study can be observed experimentally. A four roll mill device suitable for surfactant related work will be constructed to simulate a pure straining flow, based on the design of Bentley and Leal.[7] Drop deformation will be recorded using a CCD camera, allowing the shapes to be digitized and analyzed as a function of surfactant type, concentration, and applied stain rate.

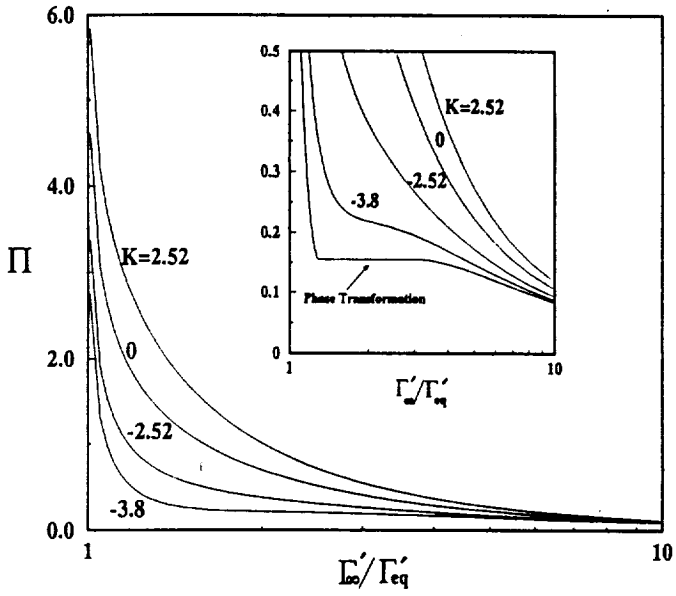

Figure 2

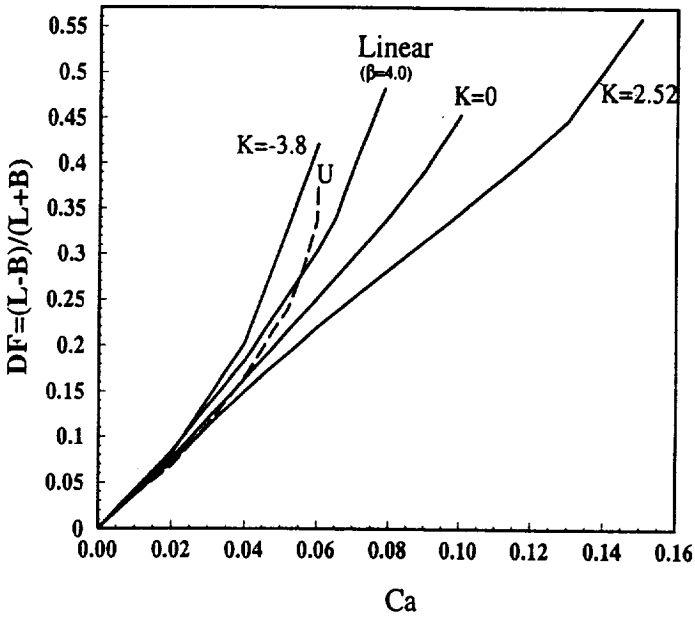

Figure 3

Bibliography

1. Stone, H. A. and Leal, L. G., J. Fluid Mech, **220,** 161 (1990)
2. Milliken, W. J., Stone, H. A. and Leal, L. G., Phys. Fluids A **5**, 69 (1993)
3. Milliken, W. J. and Leal, L. G., J. Coll. Int. Sci., **166**, 275 (1994)
4. Barthes-Biesel, D. and Acrivos, A., J. Fluid Mech, **61**, 1 (1973)
5. Rallison, J. M. and Acrivos, A., J. Fluid Mech., **89**, 191 (1978)
6.Taylor, G. I., Proc. R. Soc. London Ser., **A146**, 501 (1934)
7. Bentley and Leal J. Fluid Mech. **167**, 219 (1986)
8. Bentley and Leal J. Fluid Mech., **167**,241 (1986)
9. Levich, V.G. Physicochemical Hydrodynamics Prentice-Hall, Englewood Cliffs, N.J. (1962)
10. Fainerman, V.B. and Lylik, Kolloidnyi Zhurnal, **44**, 598 (1982)
11. Lin, S.Y., McKeigue, K. and Maldarelli, C., Langmuir **7**, 1055 (1991)
12. Johnson, D.O. and Stebe, K.J., J. Colloid Int. Sci **168**, 21-31 (1994)
13. Johnson, D.O. and Stebe, K.J., J. Colloid Int. Sci, in press
14. Pawar and Stebe, Physics of Fluids, in press
15. Unverdi, S. and Tryggvason, G. J. Comp. Phys. **100**, 25, (1992)
16. Aris, R. Vectors, Tensors, & Basic Equations of Fluid Mechanics, Prentice-Hall, Englewood Cliffs, N.J. (1962)